Preparation and Characterization of OH-Functionalized Magnetic Nanogels Under UV Irradiation

Peijun Gong,[1,2] Jiahui Yu,[1] Hanwen Sun,[1,2] Jun Hong,[1,2] Sufang Zhao,[1,2] Dongmei Xu,[1,2] Side Yao[1]

[1]*Center of Electron Beam Facilities and Radiation Processing, Shanghai Institute of Applied Physics Chinese Academy of Sciences, Shanghai 201800, China*
[2]*Graduate School of Chinese Academy of Sciences, Beijing 100039, China*

Received 4 June 2005; accepted 19 September 2005
DOI 10.1002/app.23250
Published online 14 April 2006 in Wiley InterScience (www.interscience.wiley.com).

ABSTRACT: A novel preparation method of net magnetic polymer nanogels with swollen shell was developed. UV-induced photopolymerization of 2-hydroxyethyl methacrylate (HEMA) was performed in the magnetite aqueous suspension, free of any additive to obtain monodisperse magnetic nanogels with swollen shell. Owing to the step-growth polymerization of the monomer, the particle size of magnetic nanogels can be conveniently manipulated by changing the irradiation time and the volume of the monomer dropped. The crystalline structure of Fe_3O_4 core and chemical composition of PHEMA magnetic nanogels were characterized by using X-ray diffraction, Fourier transform infrared spectroscopy, and thermogravimetric analysis, respectively. Particle sizes, size distributions of magnetic nanogels in swollen state and dry state were measured by photo-correlation spectroscopy (PCS) and transmission electron microscopy (TEM), respectively. The morphology of swollen magnetic nanogels and that of polymer capsules obtained from magnetic nanogels etched by hydrochloride acid were observed by TEM. The high magnetizations and superparamagnetic behaviors of naked Fe_3O_4 and magnetic nanogels at room temperature were confirmed by the measurement of hysteresis curves. © 2006 Wiley Periodicals, Inc. J Appl Polym Sci 101: 1283–1290, 2006

Key words: magnetic polymers; gels; photochemistry; step-growth polymerization; swelling

INTRODUCTION

Magnetic nanogels are nanosized magnetic polymer particles with core–shell structure, which are composed of magnetic cores and crosslinked polymer gel shells. The gel shell is a swelling macromolecular network with unique structure and a large amount of solvent in it. Different surface functional groups can be obtained conveniently when different monomers are used in the polymerization process. Moreover, the oxidation, acid erosion, and aggregation of superparamagnetic Fe_3O_4 particles can be weakened when Fe_3O_4 is encapsulated in the protective polymer shell.

Magnetic nanogels have attracted much attention for many years because of their great potential applications in the fields of biotechnology and biomedicine, such as enzyme immobilization, RNA/DNA purification, biosensors, immunoassays, magnetic targeted drug carriers, magnetic resonance imaging (MRI) contrast agents, and hyperthermia.[1–8] Removal of toxic metal elements and dyes in industrial wastes is also a promising application of magnetic nanogels.[9,10]

Numerous methods have been developed to prepare magnetic polymer composites with core–shell structure, including emulsion polymerization, dispersion polymerization, and surface-initiated radical polymerization.[1,11–13] However, it is not easy to obtain net magnetic nanogels with the conventional thermochemical polymerization methods, in which the surfactants and initiators are usually involved. The residual of toxic additives in the final products limits the special applications of magnetic nanogels in biomedical fields.

Photopolymerization of various monomers in alcohol can be also initiated by ultrasmall semiconductor particles.[14,15] It has also been reported by Stroyuk et al. that colloidal semiconductor nanoparticles turned out to be efficient photoinitiators of butylmethacrylate polymerization in alcohol system via a free radical process.[16]

Presently a novel approach to synthesize superparamagnetic nanogels has been proposed via photochemical reactions at room temperature in an emulsion and initiator free aqueous system in our group, via which

Correspondence to: S. D. Yao (sideyao@sinap.ac.cn).
Contract grant sponsor: Shanghai Municipal Commission for Special Project of Nanometer Science and Technology; contract grant number: 0452nm068.
Contract grant sponsor: Exploration Project of Knowledge Innovation Program of Chinese Academy of Sciences; contract grant number: 90120310.

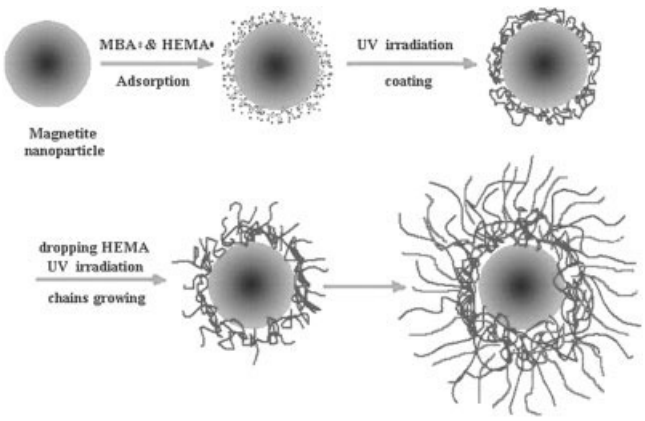

Figure 1 Schematic representation for the synthesis of OH-functionalized magnetic nanogels by photochemical approach.

the poly (acrylamide) magnetic nanogels were prepared. After Hoffmann degradation, the nanogels with amino groups were obtained and used as magnetic targeted radiopharmaceutical carriers.[17]

In this study, a one-pot photopolymerization reaction was developed to prepare OH-functionalized magnetic nanogels by using 2-hydroxyethyl methacrylate as monomer (Fig. 1), and characterized by using X-ray diffraction (XRD), Fourier transform infrared spectroscopy (FTIR), thermogravimetric analysis (TGA), photo-correlation spectroscopy (PCS), and transmission electron microscopy (TEM), respectively. The magnetic properties of magnetic nanogels at room temperature were also characterized by the measurement of hysteresis curves.

EXPERIMENTAL

Materials

2-Hydroxyethyl methacrylate (HEMA) purchased from Acros was vacuum distilled. *N*,*N*′-methylenebis(acrylamide) (MBA) served as crosslinker was recrystallized prior to use. All other chemicals were of analytical grade from Shanghai Chemical Reagents Company (China), and used without further purification, including ferric chloride hexahydrate ($FeCl_3 \cdot 6H_2O$), sodium sulfite (Na_2SO_3) and ammonium hydroxide (25% [w/w]). An 8 W low-pressure mercury lamp array was used as UV light source (Fig. 2). Pure N_2 (99.99%) were used as protective gas from oxygen during the experiment. Pure water was used as solvent.

Preparation of Fe_3O_4 nanoparticles

Superparamagnetic Fe_3O_4 was synthesized by reduction-coprecipitation method. Ferric chloride (6.49 g) was dissolved with 100 mL pure water, and charged into a 500 mL three-necked flask. N_2 was bubbled throughout the preparation process. Then, 50 mL of 0.16*M* sodium sulfite solution was slowly added into the flask. After the solution in the flask turned from red to yellow, diluted ammonia, prepared with 12 mL of concentrated ammonia and 40 mL pure water, was rapidly injected into the flask with vigorous stirring. The reaction was kept at 70°C for 30 min, and maturated for 2 h at room temperature. The black precipitate was separated by a magnet and washed several times with pure water until a pH of 7.0 was obtained. The slurry was at last dispersed in pure water.

Preparation of PHEMA magnetic nanogels

PHEMA magnetic nanogels were prepared by UV irradiation in a 100 mL three-necked quartz flask equipped with an anchor stirrer and a N_2 inlet at room temperature. The flask was fixed at the middle of the space between two parallely placed low-pressure mercury tube lamps (8 W, Philips Ltd.; major spectral energy distribution at 254 nm) apart by a distance of 10 cm (Fig. 2).

The process is as follows: the ferrofluid synthesized as mentioned earlier was sonicated for few minutes, and then 1 mL of ferrofluid (containing 6.8 mg Fe_3O_4) was introduced into the flask containing 40 mL aqueous solution of HEMA (50 μL) and MBA (5 mg). The system was stirred and bubbled with N_2. After 20 min, the mixture was exposed under UV irradiation for 4 min. Then 10 mL of water containing 450 μL HEMA was added dropwise to the flask, the mixture was kept with irradiation and agitation for another 10 min. The PHEMA magnetic nanogels were at last recovered from the reaction system by placing the flask on a permanent magnet and washed several times with pure water. The samples for FTIR, XRD, and VSM measurements were prepared by drying the net magnetic nanogels in a vacuum drier at 25°C.

Characterization

Fourier transform infrared spectroscopy (FTIR) spectra of both unmodified and modified magnetic nano-

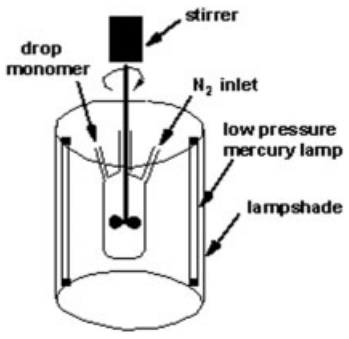

Figure 2 Schematic illustration of the photo-reactor.

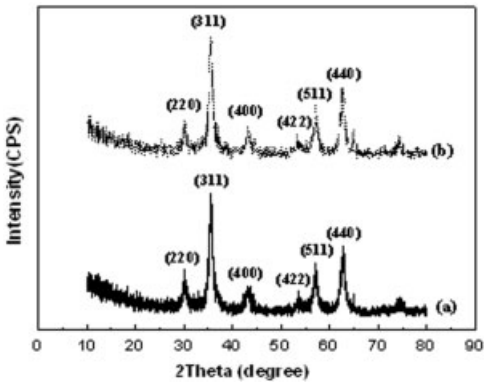

Figure 3 X-ray diffraction patterns of (a) Fe_3O_4 nanoparticles and (b) PHEMA nanogels.

particles were recorded on a FTIR spectrophotometer (Nicolet) with a KBr pellet. X-ray diffraction measurements (XRD) were performed on an X-ray diffractometer (Rigaku, Cu Kα radiation, $\lambda = 0.1542$ nm). Thermogravimetric analyses (TGA) were done by heating a 10.9 mg sample from room temperature to 600°C under N_2 atmosphere at a heating rate of 10 K min^{-1}, with a thermal analyzer (ZSCH STA 409). The morphology of magnetic nanogels were observed using a transmission electron microscope (TEM, PHILIPS CM120) at 80 kV, and the average particle size in dry state was calculated from five TEM images. Mean hydrodynamic diameters and diameter distributions were measured by a particle size analyzer (Malvern 3000HS Zetasizer) with photo correlation spectroscope (PCS) analysis at 25°C. Magnetic measurements were recorded on a vibrating sample magnetometer (VSM, Princeton Applied Research Model 155) at 25°C.

RESULTS AND DISCUSSION

Characterization of Fe_3O_4 nanoparticles

The magnetic nanoparticles were prepared by partial reduction of ferric ion by using sodium sulfite as a moderate reducing agent and succeeding coprecipitation by diluted ammonium hydroxide. The morphology of Fe_3O_4 particles was nearly spherical, and the mean size was about 14 ± 1 nm, according to the TEM image. The X-ray diffraction pattern of Fe_3O_4 nanoparticles is shown in Figure 3(a), which was in accordance with those of standard XRD data cards of Fe_3O_4 crystal (JCPDS No.19–0629). The mean diameter calculated from the XRD pattern in Scherrer formula[18] was about 13 nm, which was consistent with the result of TEM in error range. Figure 4(a) shows the magnetization curve of Fe_3O_4 nanoparticles. Superparamagnetism of Fe_3O_4 nanoparticles was confirmed by the high value of saturation magnetization (66.3 emu g^{-1}), low remanent magnetization (0.34 emu g^{-1}), and immeasurable coercivity ($\approx$ 0 Oe) (Table I).

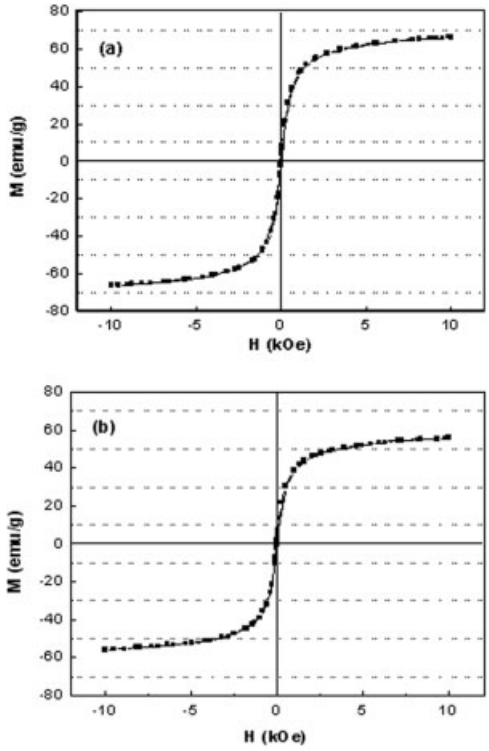

Figure 4 Hysteresis curves of (a) Fe_3O_4 nanoparticles and (b) magnetic nanogels (at 25°C).

Preparation of magnetic nanogels

The PHEMA magnetic nanogels were prepared in aqueous medium by UV photopolymerization. The process is represented in Figure 1. Fe_3O_4 nanoparticles, crosslinker MBA and monomer HEMA were mixed in a quartz flask. HEMA and MBA could be adsorbed on the surface of Fe_3O_4 primarily where the concentration of monomer was much larger than that in water. The molar extinction coefficient (åe) of Fe_3O_4 at 254 nm was much larger than those of HEMA and MBA, so when the system was exposed to UV light ($\lambda = 254$ nm), the surface of Fe_3O_4 nanoparticles was thought to absorb a majority of photons and the vinyl molecules were excited and polymerized. Meanwhile, OH radical produced from photo-catalysis of Fe_3O_4 could also initiate the polymerization of monomer adsorbed on the surface of Fe_3O_4. Therefore, it was

TABLE I
Magnetic Properties of Magnetite Particles and Magnetic Nanogels

	Sample	
	Fe_3O_4 nanoparticles	Magnetic nanogels
M_s (emu g^{-1})	66.3	55.5
M_r (emu g^{-1})	0.34	1.18
H_c (Oe)	$\approx$0	14

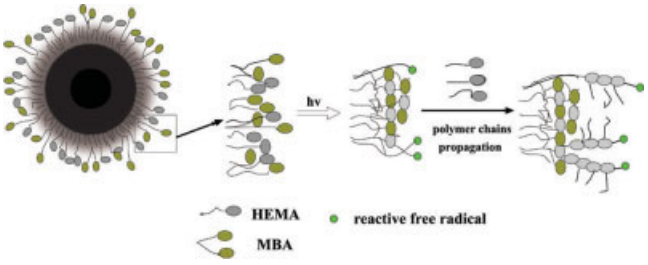

Figure 5 A schematic representation of UV initiation and polymerization and crosslinking of the individual vinyl molecules to a spherically closed polymer shell. [Color figure can be viewed in the online issue, which is available at www.interscience.wiley.com.]

assumed that polymerization of HEMA and MBA adsorbed by magnetic nanoparticles was initiated on the surface of Fe_3O_4. So Fe_3O_4 nanoparticles were coated by a thinner and tighter crosslinked net because of a relatively high ratio of crosslinker to monomer (1 : 10 w/w) at the first stage of the reaction. Figure 5 illustrates the process of UV initiation and polymerization and crosslinking of the individual vinyl molecules to spherically closed polymer shell. At the second stage, polymer chains began growing on the crosslinked layer by radical polymerization when HEMA solution was dropped continuously. As a result, the outer layer of the shell was made up of a quantity of polymer chains, and crosslinking among polymer chains might be reduced due to low ratio of crosslinker to monomer in this process. Based on the assumption mentioned earlier, we could expect that one nanogel particle contains only one Fe_3O_4 particle, and magnetic nanogels with high magnetite content could be prepared by adjusting the irradiation time and the volume of monomer dropped, which is supported by the PCS data and TEM images.

The effect of variation of irradiation time on mean hydrodynamic diameter and diameter distribution of magnetic nanogels was evaluated by PCS (Fig. 6). The mean diameter had increased from 69.0 to 186.0 nm in 10 min while 450 μL of HEMA was added dropwise into the flask. This result indicated that the thickness of polymer shell had been increasing continuously at the second stage because HEMA was involved in chain propagation on the surface of magnetic nanogels (shown as eq. (1)). A slow increasing trend (i.e., from 186.0 to 208.0 nm) was observed when a further irradiation for 20 min was performed. In fact, absorbing a minority of photons, a little part of monomer and crosslinker in aqueous solution should be polymerized upon UV light at the first stage to produce linear copolymer or crosslinked polymer particles (eq. (3)), in which the chain propagation could also occur and compete with the process on the surface of magnetic nanogels at the second stage. In eqs. (2) and (4), magnetic nanogels and polymer particles were formed as recombination of the radical on them and small monomer radical causes termination. As a result, it made the viscosity of suspension to increase and made chain propagation on the shell of magnetic nanogels to decrease. At the same time, little of the radical of polymer particles in solution might combine with each other or with the radical of magnetic nanogels to form bigger particle complexes (eqs. (4) and (5)), which were obviously observed in our experiment if irradiation time was over 30 min. The collision and deactivation of radical of magnetic nanogels could also result in the formation of magnetic nanogel complexes (eq. (6)), which was observed by TEM. The possible reaction mechanism at the second reaction stage of magnetic nanogel can be illuminated with the following equations:

$$FeM_x^{\cdot} + nM \rightarrow FeM_{x+n}^{\cdot} \text{ (the growth of magnetic nanogels)} \quad (1)$$

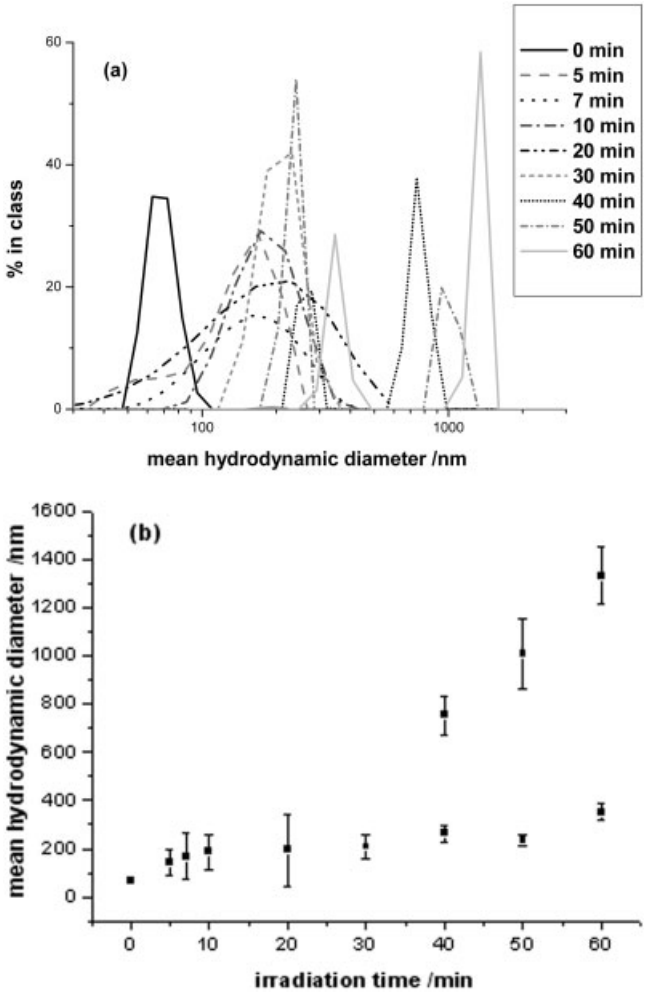

Figure 6 Effect of irradiation time on the mean hydrodynamic diameter and diameter distribution of the magnetic nanogels [V_{HEMA} (dropped) = 450 μL]: (a) diameter distribution curves by PCS; (b) dependence of mean hydrodynamic diameter (the dark point) and width of the distributed peak (the line segment) on irradiation time.

$$FeM_x^{\cdot} + nM^{\cdot} \rightarrow FeM_{x+n} \text{ (the formation of magnetic nanogels)} \quad (2)$$

$$HM_x^{\cdot} + nM \rightarrow HM_{x+n}^{\cdot} \text{(the growth of polymer particles)} \quad (3)$$

$$HM_{x+n}^{\cdot} + HM_{x+n}^{\cdot} \rightarrow HM_{x+n}\text{—}HM_{x+n} \text{ (the formation of polymer particle complexes)} \quad (4)$$

$$FeM_{x+n}^{\cdot} + HM_{x+n}^{\cdot} \rightarrow FeM_{x+n}\text{—}HM_{x+n} \text{ (the formation of magnetic nanogel complexes)} \quad (5)$$

$$FeM_{x+n}^{\cdot} + FeM_{x+n}^{\cdot} \rightarrow FeM_{x+n}\text{—}FeM_{x+n} \text{ (the formation of magnetic nanogel complexes)} \quad (6)$$

where $M^{\cdot}$, $HM_x^{\cdot}$ (or $HM_{n+x}^{\cdot}$), $FeM_x^{\cdot}$ (or $FeM_{x+n}^{\cdot}$) represent radicals of monomer, polymer particles, and magnetic nanogels respectively, and M, FeM_{x+n}, HM_{x+n} —HM_{x+n} and FeM_{x+n} —FeM_{x+n} (or FeM_{x+n} —HM_{x+n}) denote monomer molecule, magnetic nanogel, polymer particle complex, and magnetic nanogel complex, respectively.

Because complex reaction occurred in situation of longer irradiation time mentioned earlier, 10 min was selected as suitable irradiation time at the second stage in our study.

Based on the chosen irradiation time, the particle size of magnetic nanogels could be conveniently manipulated by adjusting the volume of HEMA dropped at the second stage [V_{HEMA} (dropped)]. Mean hydrodynamic diameter of magnetic nanogels (measured by PCS) ranged from 79.6 to 208.9 nm when V_{HEMA} (dropped) was adjusted from 0 to 500 μL (Fig. 7). It should be noted that the increase in diameter is about 11 nm when nanogel particles are irradiated for 10 min without HEMA dropped, which is much smaller than those with the addition of HEMA. This phenomenon gives us two indications: (1) despite no HEMA added, magnetic nanogels grow in the second stage because MBA and HEMA are not exhausted in the first stage; (2) chain propagation on the shell of magnetic nanogels takes mainly place in the second stage when HEMA is dropped into the system.

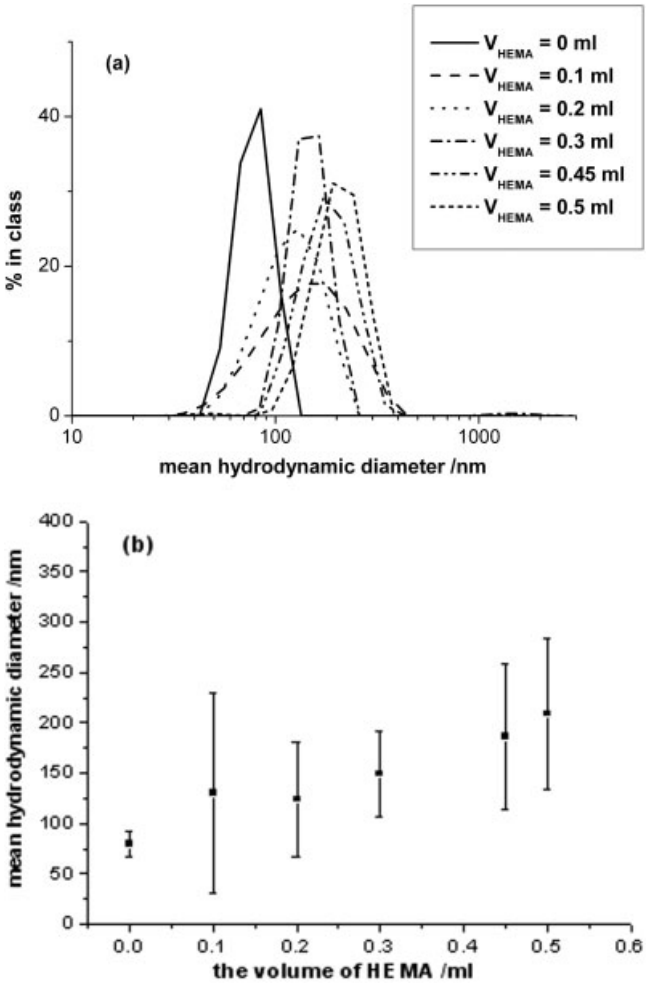

Figure 7 Effect of the added volume of HEMA on the mean hydrodynamic diameter and diameter distribution of the magnetic nanogels [irradiation time = 10 min]: (a) diameter distribution curves by PCS; (b) dependence of mean hydrodynamic diameter (the dark point) and width of the distributed peak (the line segment) on V_{HEMA} (dropped).

Chemical composition of PHEMA nanogels

Figure 8 shows the FTIR spectra of Fe_3O_4 nanoparticles (a) and PHEMA magnetic nanogels (b). The existence of PHEMA shell was confirmed by the appearance of the characteristic bands of ester bonds ($\nu_{C=O}$, 1727 cm^{-1}, ν_{C-O}, 1158 cm^{-1}), hydroxyl (ν_{O-H}, 3600–3200 cm^{-1}) and saturated C—H vibration(2960 cm^{-1} and 1455 cm^{-1}) in curve (b). The bands at 1624 and 3396 cm^{-1} in curve (a) were assigned to the bending vibration of NH_2 groups and the stretching vibration of OH groups on the surface of Fe_3O_4 nanoparticles, respectively.[19]

The XRD pattern for PHEMA magnetic nanogels is shown in Figure 3(b). The position and relative intensity of six characteristic peaks (2θ = 30.1, 35.4, 43.2, 53.4, 57.1, and 62.7°) were consistent with the literature.[20] The differences between curves in Figures 3(a) and 3(b) are negligible, which indicates that the crystal phase of Fe_3O_4 was not changed by UV irradiation.

The TG curve of magnetic nanogels is shown in Figure 9. The 2.8% weight loss of magnetic nanogels

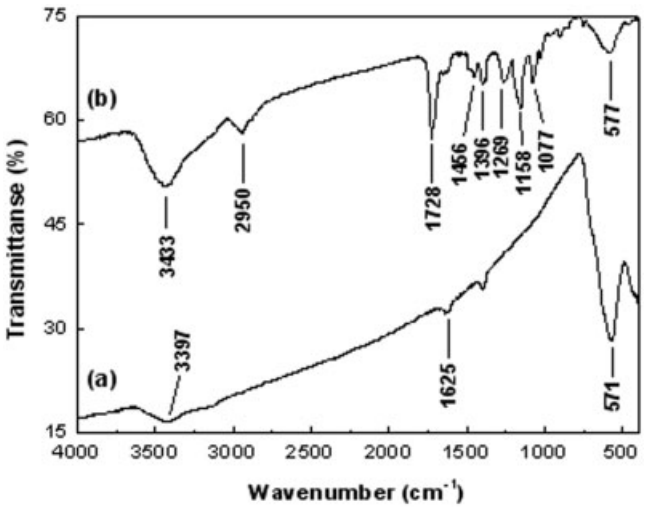

Figure 8 FTIR spectra of (a) Fe_3O_4 nanoparticles and (b) PHEMA magnetic nanogels.

was observed when the temperature rose from room temperature to 120°C, which indicated the 2.8% water content in magnetic nanogels. A 7.7% weight loss of organic material occurred from 100 to 450°C, and then a platform appeared. This indicated that the Fe_3O_4 content of magnetic nanogels in dry state was 92%. The good magnetic sensitivity was guaranteed by the high magnetite content of magnetic nanogels.

Size and morphology of magnetic nanogels

The mean hydrodynamic diameter of magnetic nanogels was analyzed as 186.0 nm, with a polydispersity index of 0.327 (Fig. 7, cyan curve; [V_{HEMA} (dropped) = 450 μL, irradiation time = 10 min]). The TEM samples were treated by different methods. Figure 10(a) was the image of magnetic nanogels dried in vacuum at room temperature, which indicated that nanogel particles with a particle size of 16 ± 2 nm aggregated because of the strong magnetic interactions. There is a noticeable discrepancy that the particle size from the TEM image is far smaller than that from the PCS analysis. Since the thickness of the swollen polymer shell is determined greatly by its dispersant, it is reasonable for the polymer shell to shrink at the surface of the magnetite as the associated water is vaporized when drying. An image of swollen magnetic nanogels was obtained by the process in which the sonicated magnetic nanogels were immediately freeze-dried in vacuum at −197°C (liquid N_2) [Fig. 10(b)]. Figure 10(b) shows typical core-shell magnetic nanogels with a particle size of 180 ± 30 nm, in good agreement with the diameter from PCS within the experimental error. The hydrated polymer shell was frozen instantaneously in liquid N_2 before shrinking, and its morphology was kept as original at a low temperature while the associated water was pumped out. Therefore, the TEM image [Fig. 10(b,c)] represents an approximate morphology of magnetic nanogels in water medium. It was noticeable that for most magnetic nanogels one nanogel particle contained only one Fe_3O_4 particle. This may be a good proof for the former assumption that polymerization of HEMA and MBA is induced on the surface of Fe_3O_4. As for a few bigger nanogels with two cores, it is considered that two nanogels collide and agglutinate to form a magnetic nanogels complex mentioned as shown in eq. (6).

For a further investigation of the morphology of the swollen polymer shell without the core, the third TEM sample [Fig. 10 (d)] was prepared as follows: hydrochloride acid (6*M* HCl) was dropped into the suspension of magnetic nanogels to etch the core till no magnetic fraction is collected by the external magnetic field, and freeze-dried the sonicated suspension at –197°C. Figure 10(d) exhibits the morphology of the polymer shell with hairy surface. It was obvious that polymer chains curled heavily on the surface of the capsules, which were darker than the shells of nanogels in Figure 10(c). These capsules with a diameter of 60 nm were much smaller than nanogels in Figure 10(c), but their interior diameter (about 25 nm) was larger than the size of Fe_3O_4. As a result of Fe_3O_4 etched by HCl, polymer capsules were dispersed in salt solution (Fe^{2+}, Fe^{3+}, and Cl^-) and the sharp discrepancy in the outside diameter was due to the fact that salt solution changed the double electric layer, and hydroxyl groups on polymer chains were inclined to coordinate ferric and ferrous ions, which resulted compression of the shell. Without the affinity between magnetite and polymer, the polymer shell swelled in water, so a cavity with a large diameter (25 nm) was formed inside polymer shell. A higher ferric and ferrous concentration in the polymer capsules made them darker in TEM image.

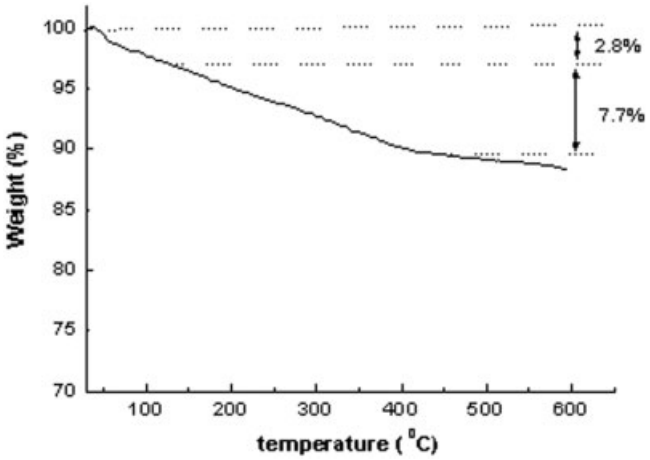

Figure 9 TGA of magnetic nanogels.

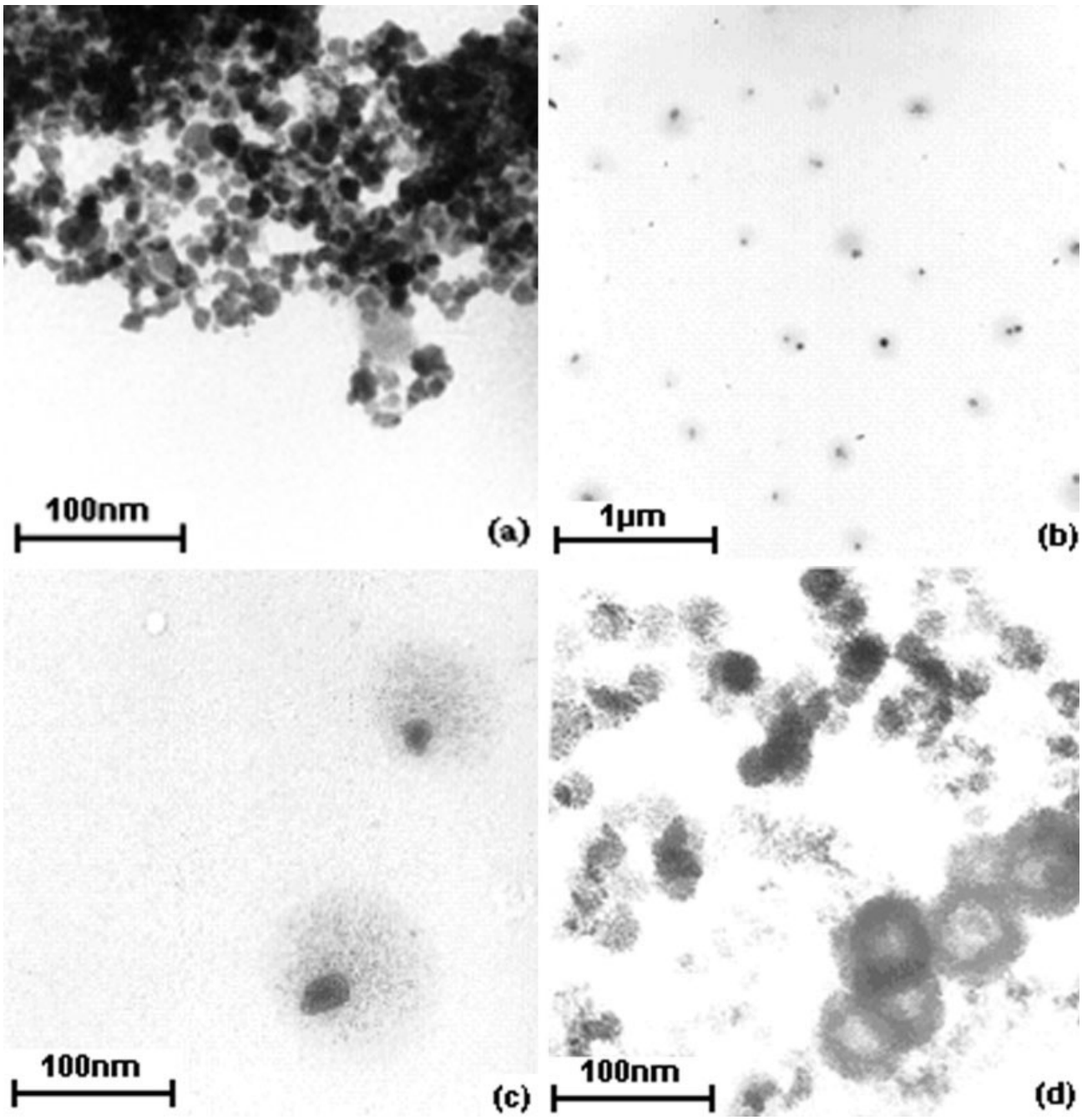

Figure 10 TEM images: magnetic nanogels dried (a) at room temperature and (b) freeze-dried in liquid N_2; (c) a magnified image of (b); and (d) hairy polymer shells.

Magnetic properties

Magnetic nanogels exhibit a good response in a magnetic field and are fully collected from water suspension by a permanent magnet in 1 min. Magnetization curves of naked Fe_3O_4 and magnetic nanogels are illustrated in Figure 4. The hysteresis curves measured for both samples showed no hysteresis and were completely reversible at 25°C. The saturation magnetization (M_s), remanent magnetization (M_r) and coercivity (H_c) were showed in Table I. It has been known that the condition for superparamagnetism is $KV \approx kT$, where KV is the anisotropy energy and kT is the thermal agitation energy. When the size of an ultrafine magnetic crystallite is below a critical number, it has only one magnetic domain and shows no magnetism in zero magnetic fields, namely behaving superparamagnetic. The size of magnetic nanoparticles in this study was below to the estimated critical number (25 nm).[21] In addition, from such low value as M_r and H_c, it was

confirmed that naked Fe_3O_4 and magnetic nanogels behaved superparamagnetic at room temperature. The saturation magnetization of PHEMA magnetite nanogels was smaller than that of the magnetite by a factor of 16%. The formation of the PHEMA shell contributed as a nonmagnetic component to the total sample mass. Another tendency towards lower magnetization may be the oxidation of the magnetite surface during the polymerization process, which leads to the formation of a trace amount of maghemite. Saturation magnetization of bulk maghemite (76 emu g^{-1}) is lower than that of bulk magnetite (92 emu g^{-1}).

CONCLUSIONS

The net PHEMA magnetic nanogels were synthesized in an aqueous system free of any additive by a photochemical method. The particle size can be easily adjusted by controlling the irradiation time and the volume of monomer dropped. TEM images confirmed the typical core-shell structure and hairy surface of magnetic nanogels. Each nanogel particle contained only one magnetite particle. Furthermore, comparisons between PCS and TEM indicated that the polymer shell had a strong swelling capability. Superparamagnetism brought magnetic nanogels a potential to biological application.

References

1. Horák, D.; Rittich, B.; Šafár, J.; Španová, A.; Lenfeld, J.; Beneš, M. J. Biotechnol Prog 2001, 17, 447.
2. Dyal, A.; Loos, K.; Noto, M.; Chang, S. W.; Spagnoli, C.; Shafi, K. V. P. M.; Ulman, A.; Cowman, M.; Gross, R. A. J Am Chem Soc 2003, 125, 1684.
3. Zhao, X.; Tapec-Dytioco, R.; Wang, K.; Tan, W. Anal Chem 2003, 75, 3476.
4. Katz, E.; Willer, I.; Wang, J. Electroanalysis 2004, 16, 19.
5. Khng, H. P.; Cunliffe, D.; Davies, S.; Turner, N. A.; Vulfson, E. N. Biotechnol Bioeng 1998, 60, 419.
6. Portet, D.; Denizot, B.; Rump, E.; Hindre, F.; Jeune, J. J. L.; Jallet, P. Drug Dev Res 2001, 54, 173.
7. Kim, E. H.; Lee, H. S.; Kwak, B. K.; Kim, B. K. J Magn Magn Mater 2005, 289, 328.
8. Chatterjee, J.; Bettge, M.; Haik, Y.; Chen, C. J. J Magn Magn Mater 2005, 293, 303.
9. Yamaura, M.; Camilo, R. L.; Felinto, M. C. F. C. J Alloys Compd 2002, 344, 152.
10. Mak, S. Y.; Chen, D. H. Dyes Pigments 2004, 61, 93.
11. Zheng, W.; Gao, F.; Gu, H. J Magn Magn Mater 2005, 288, 403.
12. Matsuno, R.; Yamamoto, K.; Otsuka, H.; Takahara, A. Macromolecules 2004, 37, 2203.
13. Marutani, E.; Yamamoto, S.; Ninjbadgar, T.; Tsujii, Y.; Fukuda, T.; Takano, M. Polymer 2004, 45, 2231.
14. Hoffman, A. J.; Yee, H.; Mills, G.; Hoffmann, M. R. J Phys Chem 1992, 96, 5540.
15. Hoffman, A. J.; Mills, G.; Yee, H.; Hoffmann, M. R. J Phys Chem 1992, 96, 5546.
16. Stroyuk, A. L.; Granchak, V. M.; Korzhak, A. V.; Kuchmii, S. Y. J Photochem Photobiol A 2004, 162, 339.
17. Sun, H.; Yu, J.; Gong, P.; Xu, D.; Zhang, C.; Yao, S. J Magn Magn Mater 2005, 294, 273.
18. Zhou, G. Structural Chemistry; Peking University Press: Beijing, 1989; p 357.
19. Chen, D. H.; Liao, M. H. J Mol Catal B 2002, 16, 283.
20. Yamaura, M.; Camilo, R. L.; Sampaio, L. C.; Macêdo, M. A.; Nakamura, M.; Toma, H. E. J Magn Magn Mater 2004, 279, 210.
21. Lee, J.; Isobe, T.; Senna, M. Colloids Surf A 1996, 109, 121.
22. Wang, S. H.; Azuma, C. J Appl Polym Sci 1996, 62, 957.